RSC Advances

PAPER

View Article Online
View Journal | View Issue

Cite this: *RSC Adv.*, 2017, **7**, 9790

Are the experimentally observed 3-dimensional carbon honeycombs all-sp^2 structures? The dangling p-orbital instability†

Zacharias G. Fthenakis

Received 6th December 2016
Accepted 23rd January 2017

DOI: 10.1039/c6ra27833g

rsc.li/rsc-advances

Recently, Krainyukova and Zubarev [*Phys. Rev. Lett.* **116**, 055501 (2016)] reported that they observed a series of all-sp^2 3-dimensional carbon honeycomb structures with interesting storage properties. In the present study we show that these structures are unstable, reducing to honeycomb structures with sp^3 atoms at the honeycomb junctions. As we show, this instability is due to solitary electrons which occupy the unhybridized p orbitals of the junction atoms, thus violating the octet rule. These orbitals are localized and have all the features that characterize *dangling orbitals*. This instability, as well as the ability of unhybridized p orbitals to form dangling bonds, has not been reported previously.

1 Introduction

Recently, Krainyukova and Zubarev[1] reported that they observed a series of 3-dimensional (3D) all-sp^2 carbon honeycomb structures, obtained by deposition of sublimated graphite. For the identification of the structures they used low temperature electron diffraction and electron microscopy methods and they reported that the structures they found could be either random or periodic. The proposed structures are composed of zig–zag terminated graphene nanoribbon (GNR) walls, interconnected through single carbon atoms arranged along a line at the wall's junctions, as shown in Fig. 1. An important feature of these structures (which was studied and reported by the authors) is that they exhibit a high level of physical absorption of several gases, like Xe, Kr and CO_2, which makes them interesting candidates for gas or liquid storage. Moreover, these structures might be of a more general interest, since they are expected to have interesting electronic, transport (thermal and electronic), and mechanical properties, which need further investigation.

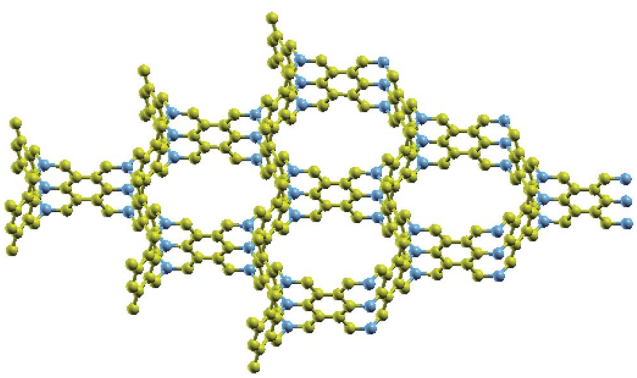

Fig. 1 A periodic representative of the 3D all-sp^2 honeycomb structure proposed by Krainyukova and Zubarev.[1] The junction atoms are shown in dark blue.

The rising interest in these structures, however, is not only because they might have interesting properties, but also because they are supposed to be the first all-sp^2 3D carbon honeycomb structures observed (and derived) experimentally. Similar 3D honeycomb structures have been proposed and studied theoretically,[2–9] but to the best of our knowledge, none of them are composed entirely of sp^2 carbon atoms. They are rather composed of sp^2 atoms at the graphitic walls and sp^3 atoms at the junctions, and they might also be random or periodic, like the structures proposed by Krainyukova and Zubarev.[1] Although these structures have not been observed experimentally, it is reported that they could be produced by collisions of graphene patches, which collide at right angles to each other, resulting in the production of Y-junctions.[9] It is worth noting, however, that other all-sp^2 3D structures, like bco-C16,[10] Rh6,[11] cR6 and cT8,[12] have been predicted theoretically, but these structures are not 3D honeycombs.

In the present study we show that the all-sp^2 3D honeycomb carbon structures proposed by Krainyukova and Zubarev[1] are unstable, reducing to mixed sp^2/sp^3 3D honeycomb structures, with the sp^3 carbon atoms at the junctions. For our calculations we utilize the density functional theory (DFT) at both the local density approximation (LDA) and the generalized gradient approximation (GGA) level. We optimize a periodic representative of these structures, shown in Fig. 1, and we show that along a transition path, which converts the unstable (proposed)

Institute of Electronic Structure and Laser, FORTH, P. O. Box 1527, 71110 Heraklio, Crete, Greece. E-mail: fthenak@iesl.forth.gr

† Electronic supplementary information (ESI) available. See DOI: 10.1039/c6ra27833g

structure to its stable counterpart, there is no energy barrier, thus leading to the conclusion that the proposed structure is unstable. It is worth noting, however, that there are studies based on phonon band structure calculations, which claim that the proposed all-sp^2 structures are stable.[13,14] In view of the results presented here, which make clear that the proposed all-sp^2 structures are unstable, the results of these studies are very difficult to rationalize.

One might assume that the instability mechanism, which is responsible for the formation of sp^2 bonds at the junctions, is similar to the mechanism which converts graphite with AA stacking to hexagonal diamond under pressure normal to the graphitic planes,[15] or the mechanism which is partly responsible for the instability of H-6 carbon.[16] However, as we show, this is not true. On the contrary, we show that this instability is due to the solitary electrons occupying the unhybridized p orbitals of the junction atoms, thus violating the octet rule. These orbitals are localized and have all the features that characterize dangling orbitals. They cannot interact with their neighboring unhybridized p electrons to form double bonds and they only have one choice for bonding: to hybridize and form single bonds with their neighboring atoms at the junctions, thus stabilizing the structure. This is not the first time that the unhybridized p-orbital orientation has been reported as being responsible for dynamic instability.[12,16]

Based on the fact that the proposed all-sp^2 structures (which were supposed to be experimentally observed) are not stable, the question which arises is what structures are these that were observed experimentally? Are they the optimized structures proposed here, or could they also be similar 3D honeycombs, like those already proposed theoretically (see for instance ref. 3 and 9)? This question, which is posed as a result of the present work, is an open question which has to be answered by experimentalists.

Based on the above, the aim of this study is (i) to make it clear that the proposed all-sp^2 structures are unstable, (ii) to act as a theoretical guide for further experimental studies on the structural properties of the 3D carbon honeycombs, (iii) to act as a warning for those intending to study the properties of these unstable structures, thus avoiding an effort which might lead to erroneous results, (iv) to show the instability mechanism which destabilizes these structures and (v) to show the ability of unhybridized p orbitals to form dangling bonds.

2 The method

All the calculations of the present study were performed using the *ab initio* DFT method as implemented by the SIESTA code,[17] utilizing both the local density approximation Ceperley–Adler functional (LDA/CA)[18] and the generalized gradient approximation Perdew–Burke–Ernzerhof (GGA/PBE)[19] functional. We use a $5 \times 5 \times 20$ Monkhorst–Pack grid[20] in the reciprocal space and a 300 Ry mesh cutoff value. For the pseudopotential of C we utilize the norm-conserving Troullier–Martins pseudopotentials[21] in the Kleinman–Bylander factorized form.[22] The basis for the wavefunction expansion in real space is an atomic-like double-zeta basis with polarization orbitals. For the structure optimizations, which include both the atomic position and lattice relaxations, we use the conjugate gradient method. The structure is considered optimized if the maximum force and stress component is smaller than 0.005 eV $Å^{-1}$ and 0.01 GPa, respectively. Using these optimization conditions, the energy accuracy of the optimized structure is less than 0.001 eV per atom.

We first consider the all-sp^2 periodic structure shown in Fig. 1. This is a periodic representative of the structures of interest and has 14 atoms per unit cell. For convenience we will call this structure "*structure A*". This 14 atom unit cell, as well as the unit cell vectors **a**, **b** and **c** of the structure, is shown in Fig. 2(a). Fig. 2(a) shows two such unit cells, each containing 2 junction atoms (one in the middle and one at the edge of the unit cell), which are shown in blue.

The periodicity of this unit cell along the **c** axis does not allow the atoms at the junction to come closer and form sp^3 pairs, as shown in Fig. 2(b). Therefore, the optimized structure A maintains its all-sp^2 character. However, if the unit cell is doubled along the **c** direction, then the formation of these sp^3 pairs is not prohibited by the periodicity of the structure. In order to find out whether or not these sp^3 pairs are formed, we optimize the structure with the doubled unit cell, as well as structure A (with the single unit cell) for comparison. As we explain in the next section, the optimized double unit cell structure prefers to form those sp^3 pairs, instead of maintaining the all-sp^2 character of structure A. The 28 atom unit cell of this optimized new structure is shown in Fig. 2(b). For convenience we will call this structure "*structure B*".

What we show next is that structure A is unstable. In order to show this, we utilize a simple transformation path that linearly transforms structure A to structure B. To construct this transformation path we consider that the unit cell of the optimized structure A is doubled along the **c** direction, so that there is a one-to-one correspondence between the atoms of the unit cell of the optimized structure A with those of the optimized structure B. The transformation path is defined by the equation

$$\mathbf{r}_i(\lambda) = \mathbf{r}_{A,i} + \lambda(\mathbf{r}_{B,i} - \mathbf{r}_{A,i}), \quad (1)$$

where $\mathbf{r}_{A,i}$ and $\mathbf{r}_{B,i}$ are the vectors describing the atomic positions of atom i in structures A and B, respectively, λ is a parameter which takes continuous values between 0 and 1, and $\mathbf{r}_i(\lambda)$ is the atomic position vector of atom i for the specific value of λ. The unit cell vectors are transformed accordingly, with the vector **c** of structure A to be doubled. Obviously, for $\lambda = 0$, the structure defined by $\mathbf{r}_i(\lambda)$ of the above equation corresponds to structure A, while for $\lambda = 1$, the structure corresponds to structure B. The same method has been used to show that H-6 carbon is unstable.[16]

3 Results and discussion

As already mentioned in the above section, we optimized both structures A and B using the DFT with both the LDA/CA and the GGA/PBE functionals. For both optimized structures the unit cell vectors have the form

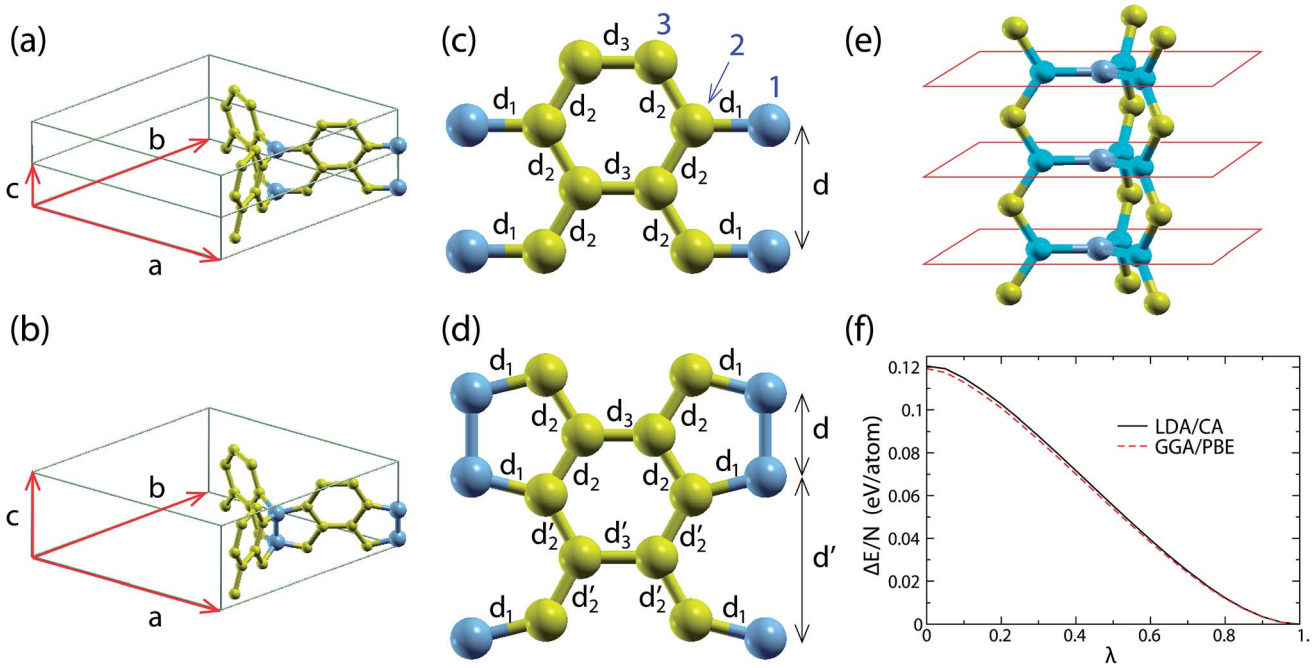

Fig. 2 (a) and (b) Unit cells of the optimized A and B structures, respectively, obtained using the LDA/CA functional. Similar structures are obtained using the GGA/PBE functional. The atoms at the junctions are shown in blue. (c) and (d) Walls of the 3D honeycombs for structures A and B, respectively. Bonds with the same bond length are shown with the same d-symbol next to them. The bond length values are shown in Table 1 of the ESI.† The atoms at the junctions are shown in blue. (e) The local planarity at the junctions of structure A. The atoms at the junctions and their first nearest neighbors are shown in dark blue and light blue, respectively. The red lines show schematically the parallel planes, which are locally graphitic with AA stacking. (f) The total energy per atom $\Delta E/N$ with respect to the corresponding energy of structure B along the transition path converting structure A to structure B (*i.e.* as a function of λ of eqn (1)).

$$\mathbf{a} = a\left(\frac{\sqrt{3}}{2}, -\frac{1}{2}, 0\right), \quad \mathbf{b} = a\left(\frac{\sqrt{3}}{2}, \frac{1}{2}, 0\right) \quad \text{and} \quad \mathbf{c} = c(0, 0, 1), \tag{2}$$

where a is the length of both $\mathbf{a}$ and $\mathbf{b}$ and c is the length of $\mathbf{c}$, *i.e.* the optimized lattice is hexagonal. The honeycomb graphitic walls are the same as each other, but the intra-wall bonds are not all the same. In Fig. 2(c) and (d) we show the different bond lengths for both of the walls of structures A and B. The symbols d_1, d_2, d_3, d'_2 and d'_3 next to each bond denote the different bond lengths, while d and d' denote the interatomic distances between the atoms at the junctions. These bond lengths, as well as the values of a and c for both structures and functionals, are shown in Table 1 of the ESI†. As we see from this table, the main structural differences between structures A and B are on the junctions.

The total energy per atom obtained from the above optimizations using the LDA/CA functional for structures A and B is $E_A^{(LDA/CA)} = -154.925$ eV and $E_B^{(LDA/CA)} = -155.045$ eV, respectively. The corresponding energy values obtained using the GGA/PBE functional are $E_A^{(GGA/PBE)} = -161.993$ eV and $E_B^{(GGA/PBE)} = -162.112$ eV. The energy differences $\Delta E_{LDA/CA} = E_B^{(LDA/CA)} - E_A^{(LDA/CA)}$ and $\Delta E_{GGA/PBE} = E_B^{(GGA/PBE)} - E_A^{(GGA/PBE)}$ are $\Delta E_{LDA/CA} = 0.121$ eV and $\Delta E_{GGA/PBE} = 0.119$ eV. Therefore, in comparison with structure A, structure B is energetically favorable, for both cases.

Moreover, calculating the energy along the transition path described in the previous section, which converts structure A to structure B, we find that the energy decreases monotonically along the transition pathway, which means that there is no energy barrier along this path. In turn, this means that structure A corresponds to an unstable equilibrium and a very small structural distortion will cause its transformation to structure B. The energy along this path, determined by the parameter λ, is shown in Fig. 2(f) for calculations with both the LDA/CA and GGA/PBE functionals. Consequently, structure A is unstable.

In order to understand the instability mechanism of structure A, let us first focus on its structural features. Structure A is planar along the graphitic walls and each junction atom is coplanar with its three first nearest neighbors (see Fig. 2(e)). The planar structure of the graphitic walls and the local planarity in the vicinity of the junction atoms give rise to sp^2 hybridization of the 2s and 2p orbitals of each C atom. The sp^2 hybridized orbitals lie along the graphitic wall planes and along the plane formed locally from each junction atom and its first nearest neighbors. The unhybridized p orbitals rise at each atom of the walls normal to the wall, and at each atom of the junctions, normal to the plane locally formed by the junction atoms and its first nearest neighbors.

Thus, due to the parallel arranged unhybridized p orbitals of the walls, each atom of the wall of structure A forms delocalized double bonds with its neighboring wall atoms, as in graphene. In contrast, the unhybridized p orbitals of the junction atoms

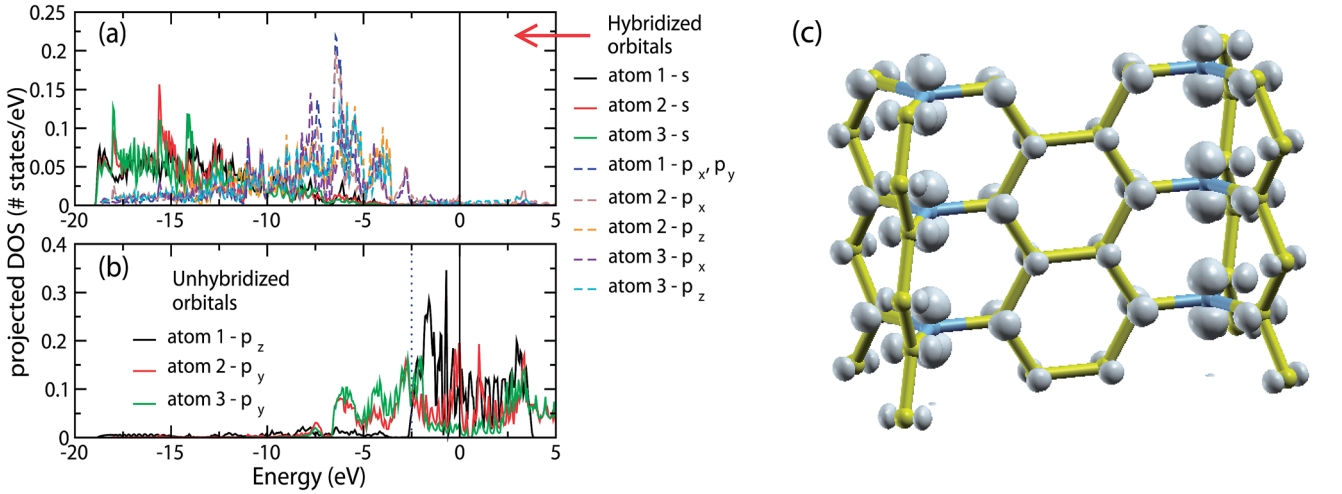

Fig. 3 (a) and (b) Partial density of states for the s and p orbitals of atoms 1, 2 and 3 (see Fig. 2(c)) of structure A. The orbitals of (a) correspond to the orbitals composing the sp^2 hybrids, while the orbitals of (b) correspond to the unhybridized p orbitals. (c) Local electron density of the electronic eigenstates with energies in the range of −2.5 to 0 eV, corresponding to the unhybridized p orbitals of the junction atoms and partly to the unhybridized p orbitals of the wall atoms.

are perpendicular to the unhybridized p orbitals of their neighboring atoms at the zig–zag edges of the walls, and therefore they do not overlap to form a bond. Thus, the atoms at the zig–zag edges of the walls form single bonds with the junction atoms‡ and the electrons occupying the unhybridized p orbitals of the junction atoms remain as solitary electrons (one electron per unhybridized p orbital), thus violating the octet rule. Therefore, these orbitals form *dangling bonds* and they are expected to be very reactive. As a consequence, the atoms at the junctions would prefer to form single bonds with each other in pairs (as in structure B) to saturate these dangling bonds, restore the octet rule and stabilize the structure.

The above picture is in agreement with the projected density of states (pDOS) of the orbitals of the atoms of structure A. In Fig. 3(a) we show the pDOS of the s and p orbitals composing the sp^2 hybrids of atoms 1, 2 and 3 shown in Fig. 2(b), while in Fig. 3(b) we show the pDOS of the corresponding unhybridized p orbitals. Due to the symmetry of the walls of structure A, only the pDOS of atoms 1, 2 and 3 are different. For the directions of p_x, p_y and p_z, we have assumed that the wall shown in Fig. 2(c) lays along the *xz* plane, with the *z*-axis along the junction line.

As we can see, the s and p orbitals composing the sp^2 hybrids contribute to the Hamiltonian eigenstates with energies in the range of −19 to −2.5 eV, laying well bellow the Fermi energy, as expected according to the picture shown in Fig. 3. The p unhybridized orbitals contribute to the Hamiltonian eigenstates with energies in the range of −7 to 0 eV, *i.e.* near the Fermi level. In particular, the pDOS of the unhybridized p orbitals of the junction atoms (atom 1 of Fig. 2(b)) corresponds to the energy range of −2.5 to 0 eV, forming a relatively narrow band. Thus, the unhybridized p orbitals of the junction atoms could interact with only those orbitals which contribute to the Hamiltonian eigenfunctions with an energy in the range of −2.5 to 0 eV. However, despite the unhybridized p orbitals of the junction atoms, only the unhybridized p orbitals of the wall atoms have significant contributions to the Hamiltonian eigenfunctions in this energy range, while the contributions of the s and p orbitals composed of the sp^2 orbitals are negligible. Recalling that the unhybridized p orbitals of the wall atoms do not interact with the unhybridized p orbitals of the junctions atoms, we come to the conclusion that the unhybridized p orbitals of the junction atoms do not interact with any of their neighboring orbitals.

However, if this was correct, the pDOS of these orbitals would be just a δ-function, located at the energy E_p of the atomic p orbitals, which does not agree with the band broadening shown in Fig. 3(b). This means that practically there are some weak interactions, which are responsible for this broadening. The most important among them are the interactions with the unhybridized p orbitals of the neighboring junction atoms, which are the second nearest neighbor interactions§ of the ppσ type. The band broadening due to these interactions can be qualitatively estimated using the tight binding approximation (TBA). Assuming interactions only between those orbitals, the energy $E(k)$ (according to the TBA) is $E(k) = E_p + 2V_{pp\sigma}(d)\cos(kd)$, where E_p is the energy of the 2p orbitals of the isolated C atom, $V_{pp\sigma}(d) = \langle 2p_z(0,0,0)|H|2p_z(0,0,d)\rangle$ is the hopping integral for the C orbitals $|2p_z(0,0,0)\rangle$ and $|2p_z(0,0,d)\rangle$ located at the positions (0,0,0) and (0,0,*d*), respectively, and *d* is the interatomic distance between neighboring junction atoms. Thus, the energy range between the lowest energy of the band ($E_p - 2|V_{pp\sigma}|$) and the Fermi level E_F ($E_F = E_p$) is $\Delta E_{1/2} - 2|V_{pp\sigma}|$. According to Papaconstantopoulos,[23] $V_{pp\sigma}(d) = V_{pp\sigma}(d_0)(d_0/d)^3$, where

‡ This explains why their bond length d_1 is so long ($d_1 \approx 1.49$ Å) in comparison with the 1.42 Å bond length of graphene at equilibrium.

§ Although junction atoms are not second nearest neighbors in terms of atom connectivity, their distance range is in the second nearest distance range, and therefore, they should be considered as second nearest neighbors.

$V_{pp\sigma}(d_0) = 0.63$ eV is the second nearest neighbor hopping integral at $d_0 = 2.525$ Å, where d_0 is the second nearest neighbor distance in diamond. Thus for $d = 2.4343$ Å in our case (according to our LDA/CA calculation), $V_{pp\sigma}(d_0) = 0.70$ eV, and therefore $\Delta E_{1/2} = 1.40$ eV. Qualitatively, therefore, this value is comparable to the corresponding 2.5 eV value of our DFT calculations, and can explain the reason for this broadening, as well as the importance of these interactions in the instability of structure A. Similar broadening occurs in the pDOS of the unhybridized p orbitals of the sp^2 terminated carbon foam surfaces,[4] due to second nearest neighbor interactions. In Fig. 3(c) we show the local electron density corresponding to the eigenstates with eigenenergies in the range of −2.5 to 0 eV, where the dominant contribution of the unhybridized p electrons of the junction atoms in this energy range is clearly shown.

To the best of our knowledge, p dangling orbitals and the corresponding instability have not been reported previously. Dangling bonds rather refer to sp^3 orbitals either on the surface of a crystalline[24,25] or in the bulk of an amorphous solid,[26] but not to unhybridized p orbitals. What is clearly shown here is that unhybridized p orbitals may also form dangling bonds.

Despite the above described instability mechanism for structure A, and taking into account that the atomic arrangement at the junctions is very similar to the structure of graphite with AA stacking, as shown schematically in Fig. 2(e), one may assume that the instability mechanism of structure A is (also) related to the mechanism that converts graphite with AA stacking to hexagonal diamond under pressure[15] and is partly responsible for the instability of H-6 carbon.[16] Indeed, this mechanism tends to buckle the structure, as it happens locally at the junctions of structure B, and therefore, the above assumption is reasonable. However, as we show in the ESI,† this is not the instability mechanism of structure A.

4 Conclusions

In the present study, using DFT calculations both at the LDA/CA and the GGA/PBE level, we show that the all-sp^2 3D carbon honeycomb structures, recently proposed by Krainyukova and Zubarev[1] as experimentally observed structures, are unstable, reducing to mixed sp^2/sp^3 3D honeycomb structures, with the sp^3 atoms at the honeycomb junctions. The instability of these structures is due to the solitary electrons occupying the unhybridized p orbitals of the junction atoms, thus violating the octet rule. These orbitals are localized and have all the features that characterize dangling orbitals. These structures are stabilized when those orbitals hybridize and form single bonds with each other in pairs, thus restoring the octet rule. To the best of our knowledge, this instability mechanism, as well as the ability of unhybridized p orbitals to form dangling bonds, has not been reported previously.

The question which is now posed, as a result of the present work, is the following: since the structure of the experimentally observed 3D carbon honeycombs is not the one proposed by Krainyukova and Zubarev,[1] what really is the internal structure of the experimentally observed 3D carbon honeycombs? Is it structure B derived from the optimization of structure A, containing not only sp^2, but also sp^3 atoms? Is it one of the other mixed sp^2/sp^3 theoretically proposed 3D honeycomb structures,[3,9] or is it a structure not yet known? This is an open question, which the experimentalists have to answer.

References

1 N. V. Krainyukova and E. N. Zubarev, *Phys. Rev. Lett.*, 2016, **116**, 055501.
2 Z. Zhu, Z. G. Fthenakis, J. Guan and D. Tománek, *Phys. Rev. Lett.*, 2014, **112**, 026803.
3 A. Kuc and G. Seifert, *Phys. Rev. B: Condens. Matter Mater. Phys.*, 2006, **74**, 214104.
4 Z. Zhu and D. Tománek, *Phys. Rev. Lett.*, 2012, **109**, 135501.
5 K. Umemoto, S. Saito, S. Berber and D. Tománek, *Phys. Rev. B: Condens. Matter Mater. Phys.*, 2001, **64**, 193409.
6 S.-Z. Chen, F. Xie, F. Ning, Y.-Y. Liu, W.-X. Zhou, J.-F. Yu and K.-Q. Chen, *Carbon*, 2017, **111**, 867–877.
7 G. Yu, L. Jiang and Y. Zheng, *Appl. Phys. Lett.*, 2014, **105**, 061601.
8 A. Martínez-Mesa, L. Zhechkov, S. N. Yurchenko, T. Heine, G. Seifert and J. Rubayo-Soneira, *J. Phys. Chem. C*, 2012, **116**, 19543–19553.
9 T. Kawai, S. Okada, Y. Miyamoto and A. Oshiyama, *Phys. Rev. B: Condens. Matter Mater. Phys.*, 2005, **72**, 035428.
10 J.-T. Wang, H. Weng, S. Nie, Z. Fang, Y. Kawazoe and C. Chen, *Phys. Rev. Lett.*, 2016, **116**, 195501.
11 J.-T. Wang, C. Chen, E. Wang and Y. Kawazoe, *Sci. Rep.*, 2014, **4**, 4339.
12 J.-T. Wang, C. Chen and Y. Kawazoe, *Sci. Rep.*, 2013, **3**, 3077.
13 Z. Yang, G. Lan, B. Ouyang, L.-C. Xu, R. Liu, X. Liu and J. Song, *Mater. Chem. Phys.*, 2016, **183**, 6–10.
14 Y. Gao, Y. Chen, C. Zhong, Z. Zhang, Y. Xie and S. Zhang, *Nanoscale*, 2016, **8**, 12863–12868.
15 S. Fahy, S. G. Louie and M. L. Cohen, *Phys. Rev. B: Condens. Matter Mater. Phys.*, 1987, **35**, 7623–7626.
16 Z. G. Fthenakis, *RSC Adv.*, 2016, **6**, 78187–78193.
17 J. M. Soler, E. Artacho, J. D. Gale, A. García, J. Junquera, P. Ordejón and D. Sánchez-Portal, *J. Phys.: Condens. Matter*, 2002, **14**, 2745.
18 D. M. Ceperley and B. J. Alder, *Phys. Rev. Lett.*, 1980, **45**, 566–569.
19 J. P. Perdew, K. Burke and M. Ernzerhof, *Phys. Rev. Lett.*, 1996, **77**, 3865–3868.
20 H. J. Monkhorst and J. D. Pack, *Phys. Rev. B: Condens. Matter Mater. Phys.*, 1976, **13**, 5188–5192.
21 N. Troullier and J. L. Martins, *Phys. Rev. B: Condens. Matter Mater. Phys.*, 1991, **43**, 1993–2006.
22 L. Kleinman and D. M. Bylander, *Phys. Rev. Lett.*, 1982, **48**, 1425–1428.
23 D. Papaconstantopoulos, *Handbook of the band structure of elemental solids*, Plenum Press, New York and London, 1986.
24 B. P. Lemke and D. Haneman, *Phys. Rev. B: Condens. Matter Mater. Phys.*, 1978, **17**, 1893–1907.
25 S. R. Schofield, P. Studer, C. F. Hirjibehedin, N. J. Curson, G. Aeppli and D. R. Bowler, *Nat. Commun.*, 2013, **4**, 1649.
26 R. Biswas, C. Z. Wang, C. T. Chan, K. M. Ho and C. M. Soukoulis, *Phys. Rev. Lett.*, 1989, **63**, 1491–1494.

